

A Computational Study on the Mechanism of Intramolecular Oxo–Hydroxy Phototautomerism Driven by Repulsive $\pi\sigma^*$ State

Bartosz Chmura, Michal F. Rode, Andrzej L. Sobolewski, Leszek Lapinski, and Maciej J. Nowak*

Institute of Physics, Polish Academy of Sciences, Al. Lotnikow 32/46, 02-668 Warsaw, Poland

Received: August 8, 2008; Revised Manuscript Received: October 22, 2008

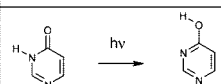
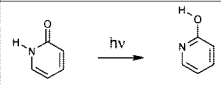
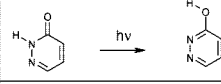
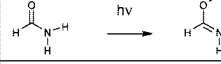
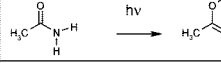
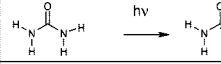
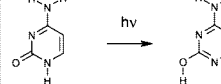
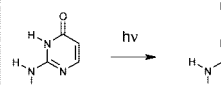
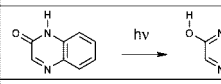
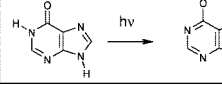
Potential energy (PE) surfaces of the lowest excited states of the 4(3*H*)-pyrimidinone/4-hydroxypyrimidine system were investigated with the aid of the CC2 and CASSCF methods of the electronic structure theory. These studies resulted in identification of a low-lying $\pi\sigma^*$ state, which is dissociative with respect to the stretching of the N–H or O–H bonds in the oxo and hydroxy structures of the compound, respectively. After initial excitation to the lowest local $n\pi^*$ and/or $\pi\pi^*$ singlet states, the system can access the PE surface of the $\pi\sigma^*$ state by crossing a low barrier. It was computationally demonstrated that the system should evolve on the PE surface of the repulsive $\pi\sigma^*$ state toward a broad seam of intersection with the PE surface of the ground state. At the intersection, the nonadiabatic transition to the ground electronic state takes place and the system can either evolve to a minimum of the initially excited tautomer or to the ground-state minimum of the other tautomer. The steps listed above provide a mechanism of photoinduced dissociation–association (PIDA) phototautomerism, experimentally observed for a number of monomeric molecules, structurally similar to 4(3*H*)-pyrimidinone/4-hydroxypyrimidine. This mechanism describes a new class of intramolecular phototautomeric reactions driven by a repulsive $\pi\sigma^*$ state.

Introduction

Photoinduced intramolecular proton-transfer processes were observed for a diversity of heterocyclic and simple amides isolated in low-temperature, inert gas matrixes. The list of representative examples of this phototautomeric process is given in Table 1. Upon exposure of the matrix-isolated monomers of these compounds to UV light, the oxo forms were generally converted into the hydroxy tautomers. This phototautomeric reaction occurred for compounds having the oxo form more stable in S_0 [e.g., 4(3*H*)-pyrimidinone/4-hydroxypyrimidine (4PMD/4HPM), where the energy difference is 2.4 kJ mol⁻¹, in favor of the oxo tautomer]⁴ as well as for compounds having the hydroxy form more stable in S_0 [e.g., 2(1*H*)-pyridinone/2-hydroxypyridine (2PD/2HP), where the energy difference is 2.9 kJ mol⁻¹, in favor of the hydroxy tautomer].⁴ Phototransformations of the hydroxy forms into the oxo tautomers were also observed, but phototautomeric reactions in this direction are less pronounced. So far there are only two well documented examples of the hydroxy \rightarrow oxo phototautomerism.^{15,16}

The intramolecular photoinduced proton-transfer reactions in compounds listed in Table 1 are fundamentally different from the well-known excited-state intramolecular proton-transfer (ESIPT) processes. In ESIPT, proton is transferred along an intramolecular hydrogen bond, which is present in the ground and in the excited-state structures of the substrate and of the photoproduct. For the compounds shown in Table 1, the acidic (proton-donating) and the basic (proton-accepting) molecular moieties are not connected by intramolecular hydrogen bonds. In effect, the oxo forms of these species are separated from the hydroxy tautomers by a barrier as high as 144–188 kJ mol⁻¹ on the potential energy (PE) surface of the ground electronic state.^{17,18} The second prerequisite of the ESIPT processes, which

TABLE 1: Photoinduced Intramolecular Proton-Transfer Processes Observed for Heterocyclic and Simple Amides Isolated in Low-Temperature Matrixes

Compound	UV-induced proton-transfer reaction	References
4(3 <i>H</i>)-pyrimidinone 4-hydroxypyrimidine		[1, 2, 3, 4]
2(1 <i>H</i>)-pyridinone 2-hydroxypyridine		[4, 5]
3(2 <i>H</i>)-pyridazinone 3-hydroxypyridazine		[6]
formamide formic acid		[7, 8]
acetamide acetimidic acid		[9]
urea isourea		[10]
cytosine		[11, 12]
isocytosine		[13]
2(1 <i>H</i>)-quinoxalinone 2-hydroxyquinoxaline		[4]
hypoxanthine		[14, 15]

* To whom correspondence should be addressed. E-mail: mjanowak@ifpan.edu.pl.

concerns lower energy of S_1 in the photoproducted tautomer with respect to the S_1 energy of the substrate, is not fulfilled for the phototautomeric processes listed in Table 1. As it was shown by the experimental studies of the fluorescence excitation spectra, recorded for jet-cooled **2PD/2HP** system, the 0–0 line in the $S_0 \rightarrow S_1$ transition appears at 29831 cm^{-1} (335.2 nm) for the oxo form and at 36136 cm^{-1} (276.7 nm) for the hydroxy form.¹⁹ The above assignment of the 0–0 transitions to the oxo and hydroxy forms, respectively, was proved by a measurement of the fluorescence excitation spectrum of 1-methyl-2(1*H*)-pyridinone, where the 0–0 line was found at 29822 cm^{-1} (335.3 nm).²⁰ Similarly, for the **4PMD/4HPM** system, the 0–0 transitions were observed at 30528 cm^{-1} (327.6 nm) for the oxo form and at 35337 cm^{-1} (283.0 nm) for the hydroxy form.²¹ Hence, the energies of S_1 states in the oxo substrates of the phototautomeric reactions are lower than the energies of S_1 states in the hydroxy photoproducts. Moreover, it was experimentally shown³ that the oxo \rightarrow hydroxy conversion in **4PMD/4HPM** occurs already upon UV ($\lambda = 308 \text{ nm}$) irradiation. Therefore, due to simple energetic reasons, the involvement of the S_1 state of the hydroxy form into the oxo \rightarrow hydroxy phototautomeric process (which would be necessary within the ESIPT mechanism) can safely be ruled out. All the reasons described above clearly show that a mechanism other than ESIPT must govern the intramolecular photoinduced proton-transfer reactions listed in Table 1.

Several years ago, it was pointed out, by one of the present authors (A.L.S.), that optically dark excited states of $\pi\sigma^*$ character play an essential role in the photochemistry of aromatic molecules with acidic groups, such as pyrrole, indole or phenol.^{22–24} The potential energy (PE) function of these $\pi\sigma^*$ states is generically dissociative with respect to the stretching coordinates of O–H or N–H bonds. The PE surfaces of the $\pi\sigma^*$ states cross with the PE surface(s) of the ${}^1\pi\pi^*$ excited state(s) as well as with the PE profile of the electronic ground state. These PE crossings, which are symmetry-allowed in the planar systems (since S_0 and ${}^1\pi\pi^*$ states transform as A' , while $\pi\sigma^*$ states transform as A''), become conical intersections when out-of-plane modes are taken into account. These intersections can provide a pathway for efficient radiationless decay to the electronic ground state as well as for hydrogen detachment.^{25,26} The photoinduced hydrogen-detachment processes, driven by repulsive $\pi\sigma^*$ states, are nowadays well understood in pyrrole, phenol, and indole. For these systems, these photoinduced processes were experimentally documented by detection of the fast hydrogen atoms, generated from the molecules promoted (by absorption of UV photons) to the low-energy excited states.^{27–35}

In the early theoretical investigations,^{36–38} aimed at elucidation of phototautomerism in **2PD/2HP**, one of us (A.L.S.) considered a role of repulsive $\pi\sigma^*$ states in cleavage of the N–H and/or O–H bonds. A mechanism based on photoinduced dissociation–association (PIDA) of hydrogen atom was postulated in those works. In the current paper, we present a computational study on the mechanism of the UV-induced intramolecular proton transfer in **4PMD/4HPM**. This study resulted in generation of a convincing PIDA model involving the following key steps: (1) hydrogen detachment driven by the repulsive $\pi\sigma^*$ state, (2) nonadiabatic relaxation to the ground state at the seam of intersection between the $\pi\sigma^*$ and S_0 states, and (3) hydrogen attachment to a vicinal heteroatom on the ground-state PE surface. The phototautomeric occurrences following this (PIDA) mechanism constitute, alongside the

TABLE 2: Vertical Excitation Energies (ΔE), Oscillator Strengths (f) and Dipole Moments (μ) of the Low-Energy Singlet Excited States of 4-Hydroxypyrimidine and 4(3*H*)-Pyrimidinone Calculated with the CC2/aug-cc-pVDZ Method at Geometries Optimized for the Ground Electronic State at the MP2/aug-cc-pVDZ Level

state	$\Delta E/\text{eV}$	f	μ/debye
4-Hydroxypyrimidine			
S_0	0.0	—	1.35
$n\pi^*$	4.84 (4.91) ^a	0.001	0.87
$\pi\pi^*$	5.28 (4.81) ^a	0.370	2.03
$\pi\pi^*$	6.36 (6.43) ^a	0.043	1.87
$\pi\pi^*$	6.41	0.090	1.90
$\pi\sigma^*$	6.67	0.00005	4.17
4(3 <i>H</i>)-Pyrimidinone			
S_0	0.0	—	3.19
$n\pi^*$	4.67 (5.20) ^a	0.0002	0.72
$\pi\pi^*$	4.74 (4.53) ^a	0.085	6.39
$\pi\pi^*$	6.00 (6.22) ^a	0.165	6.43
$\pi\pi^*$	6.14	0.025	0.98
$\pi\sigma^*$	5.90	0.0007	6.94

^a Calculated with the CASPT2(14,11)/6-31G(d,p) method at geometries optimized for the ground electronic state at the MP2/aug-cc-pVDZ level.

intramolecular ESIPT and intermolecular³⁹ photoreactions, a separate class of photoinduced proton-transfer processes.

Computational Methods

Within the current work, the energies of the electronically excited states were calculated with the CC2 method,^{40,41} making use of the resolution-of-the-identity (RI) approximation for the evaluation of the electron-repulsion integrals.^{42,43} The CC2 calculations were carried out with the TURBOMOLE program package.⁴⁴ The energies of the excited states were also calculated using the multireference CASSCF method⁴⁵ as it is implemented in the MOLPRO program package.⁴⁶ In the calculations carried out in this work, the correlation-consistent polarized valence double- ζ (cc-pVDZ) basis set and the augmented correlation-consistent polarized valence double- ζ (aug-cc-pVDZ) basis set were employed⁴⁷ as specified below.

Results and Discussion

Locally Excited States. For the oxo **4PMD** and the hydroxy **4HPM** tautomers of 4-pyrimidinone, energies of vertical electronic excitations have been calculated using the CC2, CASSCF and CASPT2 methods. These calculations were carried out for the ground-state equilibrium geometries of **4PMD** and **4HPM** optimized at the MP2⁴⁸ or CASSCF level. Results of these computations (collected in Table 2 and in Table S1 in the Supporting Information) show that the oxo **4PMD** form absorbs UV light at longer wavelengths in comparison with the absorption of the hydroxy **4HPM** tautomer. This prediction is consistent with experimental results obtained for the **4PMD/4HPM** system²¹ as well as for related compounds e.g. **2PD/2HP**.¹⁹

In the experimental studies of UV absorption spectrum of the **4PMD/4HPM** system in the gas phase,^{49,50} the maximum of the absorption band due to **4PMD** form was observed at the

wavelength corresponding to the energy of 4.51 eV. This experimental value is fairly well reproduced by the energies of vertical transitions to the lowest $n\pi^*$ and $\pi\pi^*$ states, calculated at the CC2 as well as at the CASPT2 levels. Similarly, the experimental value 4.86 eV, measured for the maximum of the absorption band of **4HPM**, is fairly well reproduced by the respective energies of vertical transitions to the lowest $n\pi^*$ and $\pi\pi^*$ states, calculated at the CC2 and CASPT2 levels (see Table 2 and Table S1 in the Supporting Information).

The energies of the $n\pi^*$ and $\pi\pi^*$ states were also calculated (using the CC2/aug-cc-pVDZ method) at the minima of these excited states. The obtained values, 3.41 eV ($n\pi^*$) and 3.93 eV ($\pi\pi^*$) for **4PMD** and 4.17 eV ($n\pi^*$) and 4.97 eV ($\pi\pi^*$) for **4HPM** (taken with respect to the energy of the ground state calculated at the optimized geometry of S_0), correspond well to the 0–0 origins of experimental bands observed at 3.78 eV for **4PMD** and at 4.38 eV for **4HPM**, in the spectra of the compound in a supersonic jet expansion.²¹ Analogously, the energies of the lowest excited $\pi\pi^*$ states of **4PMD** and **4HPM** tautomers were calculated at the CASPT2/6-31G(d,p) level, for the geometries of these states optimized at the CC2 level. The computed values of the energies of these excited, optically bright $\pi\pi^*$ states (4.10 eV or **4PMD** and 4.73 eV for **4HPM**, calculated with respect to the energy of the ground state at the optimized geometry of S_0), are overestimated by ca. 0.3 eV in comparison with the experimental energies of the 0–0 band origins.

A feature, apparent from all the results presented in Table 2 and discussed in the paragraphs above, concerns the prediction of pairs of the close-in-energy $n\pi^*$ and $\pi\pi^*$ states as the lowest-energy excited states of the oxo as well as of the hydroxy tautomers. Similar pairs of $n\pi^*$ and $\pi\pi^*$ low-energy excited states were theoretically predicted (using different methods of the electronic structure theory), for the oxo and hydroxy tautomers of such compounds as 2-pyridinone^{36–38} and 2-pyrimidinone.⁵¹ These $n\pi^*$ and $\pi\pi^*$ states are so close in energy that they are significantly immersed in each other and could be treated as separate states only for a planar geometry (C_s symmetry) of the system, since under this symmetry constraint these states transform according to A'' and A' representations, respectively. Any out-of-plane deformation of the system results in vibrationally induced coupling between the states and, in fact, the lowest excited singlet state of the system is expected to have a mixed $n\pi^*/\pi\pi^*$ character. The lowest-energy excited states of the $\pi\sigma^*$ (and $n\sigma^*$) nature are energetically higher by about 1 eV than the respective $\pi\pi^*$ and $n\pi^*$ states.

Repulsive $\pi\sigma^*$ State and Its Intersection Seam with the Ground Electronic State. In the following, we are going to provide a mechanistic overview of the PIDA reaction, where the proton detaches from the acidic moiety and then attaches to the nearby basic spot at the same molecule. Description of this reaction in terms of intramolecular coordinates would be a challenging task, since this would involve a redundant mixture of stretching and bending coordinates. Thus, we decided to describe the phenomenon in terms of Cartesian coordinates of the mobile hydrogen atom. In the Cartesian coordinate system, the molecule could be oriented in such a way that one of the axes points in the direction of the detaching hydrogen (Chart 1). Hence, in order to describe the hydrogen atom detachment from 4-pyrimidinone molecule, the movement of the H-atom in the direction of the y -axis perpendicular to the axis going through the oxygen and the nitrogen atoms (Chart 2) has to be considered. On the other hand, change of the tautomeric form, that is H-atom transfer from N(3) to O (or *vice versa*), must

CHART 1: Comparison of the Structures of Classic Examples of H-Atom Photodetachment Driven by a Repulsive $\pi\sigma^*$ State and the 4(3H)-Pyrimidinone and 4-Hydroxypyrimidine Tautomers Considered in the Current Work

Classic examples of H-atom photodetachment driven by a repulsive $\pi\sigma^*$ state

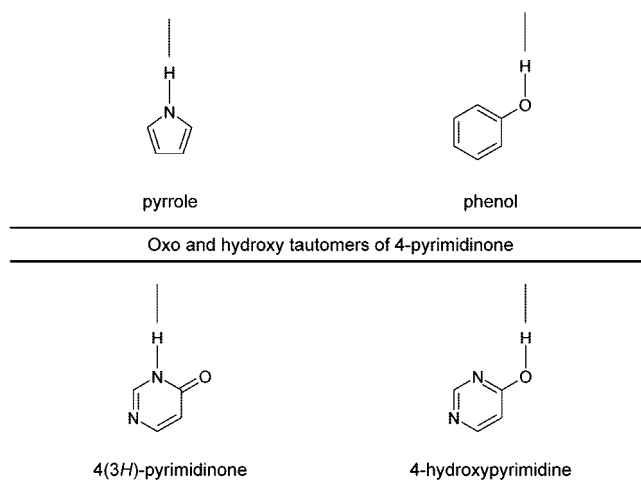
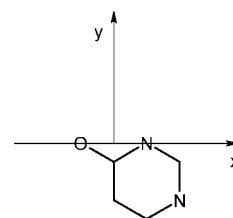


CHART 2: Orientation of the x and y Cartesian Axes Describing the Position of the Labile Proton with Respect to the Molecular Frame



involve a movement in the direction parallel to the x -axis (Chart 2) connecting the O and N(3) atoms. A point in the middle of the distance between the oxygen and nitrogen atoms (see Chart 2) was chosen as the origin of the x and y Cartesian coordinate system.

In order to map the ground- and excited-state PE surfaces in the Franck–Condon (FC) region, corresponding to the ground-state minimum of a given tautomer, the energies of the electronic states were calculated (at the CC2/aug-cc-pVDZ level) at the Cartesian grid around the ground-state equilibrium geometry. For each point of this grid, x and y coordinates determined the position of the labile hydrogen atom, whereas the values of Cartesian coordinates determining the positions of all other atoms were kept frozen at the ground-state optimized structure of the respective (oxo or hydroxy) tautomer. The obtained PE surfaces of the S_0 ground state and the $n\pi^*$ and $\pi\pi^*$ lowest excited singlet states are graphically presented in Figure 1. These results illustrate well that the minima of the locally excited $n\pi^*$ and $\pi\pi^*$ low-energy states are nearly as deep as the minima of the oxo and hydroxy tautomers on the ground-state PE surface. Hence, it does not seem possible to explain the phototautomerism experimentally observed in the **4PMD/4HPM** system, by taking only these $n\pi^*$ and $\pi\pi^*$ locally excited states into account.

Thus another, more extended scan of the PE surfaces of the ground and lowest excited states has been carried out by performing CC2/aug-cc-pVDZ calculations, for a series of points differing by x and y coordinates describing the position of the

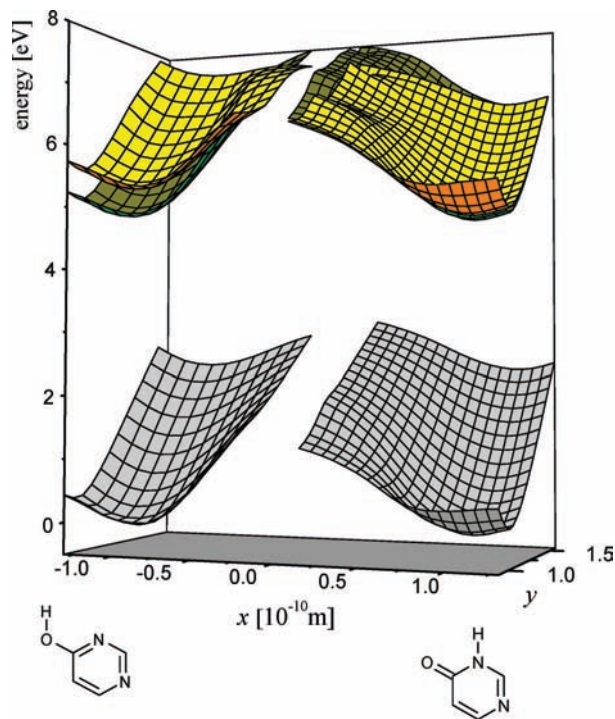


Figure 1. Potential energy surfaces of the 4(3H)-pyrimidinone/4-hydroxypyrimidine system in the ground state (gray), locally excited $n\pi^*$ state (olive) and the locally excited $\pi\pi^*$ state (yellow). The energies were calculated (at the CC2/aug-cc-pVDZ level) for the proton located at x and y coordinates (see Chart 2), while the rest of the molecule was kept at a frozen geometry optimized for the ground-state structures of the oxo and the hydroxy tautomers.

mobile proton, whereas the remaining part of the molecule was kept at the geometry optimized for the radical (with the labile hydrogen atom removed). The planarity of the system was conserved throughout all the calculations. The results of these calculations are presented in Figure 2. For transparency, in this figure the locally excited states are represented only by the lowest, optically accessible $\pi\pi^*$ singlet state. In comparison to Figure 1, a novel feature shown in Figure 2 is the PE surface of the $\pi\sigma^*$ excited singlet state. This state is repulsive with respect to detachment of the hydrogen atom and becomes the lowest excited singlet state at larger OH/NH distances. The $\pi\sigma^*$ state can be accessed from the initially populated $n\pi^*$ and $\pi\pi^*$ states by overpassing a relatively low barrier.

According to the results of the calculations presented in Figure 2, the system should evolve on the PE surface of the $\pi\sigma^*$ state toward an intersection seam with the ground electronic state. This picture is quite similar to those of the previously studied systems (such as pyrrole or phenol) known to exhibit a photoinduced H-atom detachment driven by the repulsive $\pi\sigma^*$ state. Whereas in pyrrole (or phenol) H-atom can be detached only from one N–H (or O–H) bond, in the **4PMD/4HPM** system there are two neighboring heteroatoms capable to detach or attach a labile hydrogen atom. The results of the calculations presented in Figure 2 predict that, for the **4PMD/4HPM** system, the intersection seam between the $\pi\sigma^*$ and the ground states is very extended and common for both oxo and hydroxy tautomers. This broad seam is very flat and consists of nearly isoenergetic points. From the region of this seam, the system can relax (in an essentially barrierless manner) toward one of the two ground-state minima. If the minimum populated in the course of the reaction is not the same as that of the initially excited tautomer, then UV excitation of the molecule results in a change of its tautomeric form.

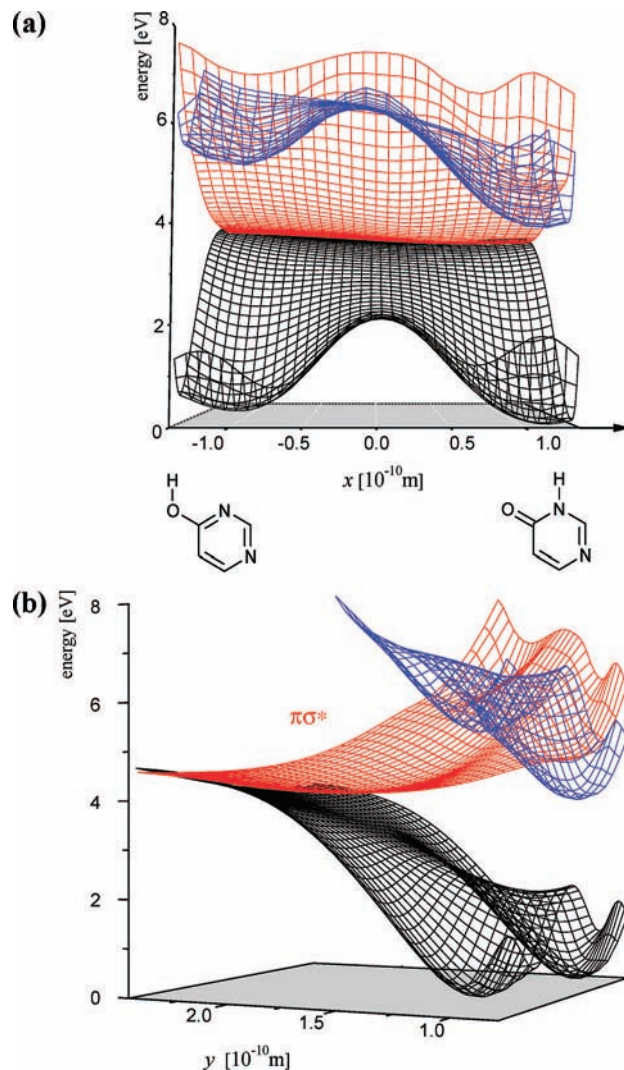


Figure 2. Potential energy surfaces of the 4(3H)-pyrimidinone/4-hydroxypyrimidine system in the ground state (black), locally excited $\pi\pi^*$ state (blue) and the repulsive $\pi\sigma^*$ state (red). The energies were calculated (at the CC2/aug-cc-pVDZ level) for the proton located at x and y coordinates (see Chart 2), while the rest of the molecule was kept at a frozen geometry optimized for the π -radical.

A single-reference method, such as CC2, is expected to fail in the vicinity of the intersection seam between an excited state and the electronic ground state. The accurate calculation of the PE surfaces in the immediate vicinity of the S_1 – S_0 intersections requires the use of multireference methods, in particular of state-averaged CASSCF and MR perturbation or configuration-interaction methods. To provide more insight into the mechanism of the phototautomeric reaction in the **4PMD/4HPM** system, we calculated (at the state-averaged CASSCF level) one-dimensional PE profiles along two linear-synchronous-transit (LST) reaction paths. One of these paths led from the ground-state minimum of the hydroxy tautomer to the seam of intersection of the $\pi\sigma^*$ and S_0 states (see Figure 3), whereas the other LST path led from the ground-state minimum of the oxo tautomer to the seam of intersection of the $\pi\sigma^*$ and S_0 states. The ground-state equilibrium geometries of the hydroxy and oxo tautomeric forms (optimized at the MP2/cc-pVDZ level of theory) were used in these calculations as terminal points. The third terminal structure, which was the same in both LST paths, was a point where the mobile hydrogen atom was placed at the y axis and the OH and NH distances were equal to 2.05 Å. All other geometry parameters characterizing this point were kept

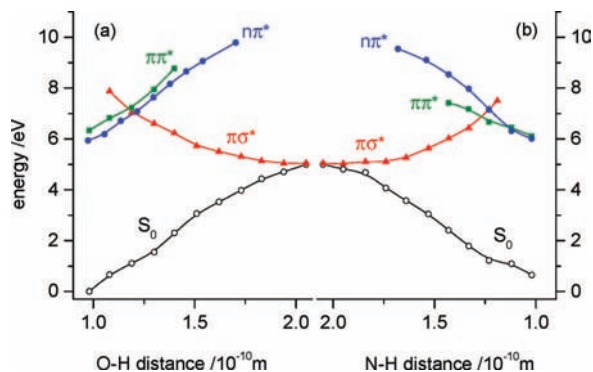


Figure 3. Potential energy profiles of the ground and excited electronic states of the 4(3H)-pyrimidinone/4-hydroxypyrimidine system. Energies were calculated at the CASSCF(14,11)/cc-pVDZ level for geometry points along the linear-synchronous-transit (LST) reaction paths leading from the ground-state minima of (a) hydroxy, (b) oxo tautomers to the point characterized by OH and NH distances equal to 2.05 Å.

as they were optimized at the MP2 level for the radical. It was computationally demonstrated that for this geometry the energies of the $\pi\sigma^*$ and S_0 states [calculated at the CASSCF(14,11)/cc-pVDZ level] are nearly the same, whereas for other values of the OH = NH distances the calculated energies of the $\pi\sigma^*$ and S_0 states were clearly distinct. Hence, the geometry point characterized by the OH and NH distances equal to 2.05 Å could serve as a good representative point belonging to the extended seam of intersection of the $\pi\sigma^*$ and S_0 states.

In the LST approach, all internal coordinates (bond lengths and bond angles) are varied in a proportional manner from one terminal structure (the ground-state equilibrium geometry of a given tautomer) to the other terminal structure (geometry point with significantly elongated OH and NH distances of 2.05 Å each). Along this reaction path, single-point energy calculations of the ground state and the lowest excited singlet states ($\pi\pi^*$, $n\pi^*$, and $\pi\sigma^*$) have been performed at the CASSCF(14,11)/cc-pVDZ level. More details concerning the LST approach can be found in ref 52.

In the single-point CASSCF calculations carried out along the LST, a balanced description of states with different electronic structure is required. That is why we employed a fairly large active space consisting of 14 electrons correlated over 11 molecular orbitals. This active space includes six π orbitals, three lone pair orbitals (n), and two σ^* orbitals. The CASSCF calculations have been performed with the MOLPRO program package.⁴⁶

The PE profiles calculated at the CASSCF level are shown in Figure 3. On inspection of these results, one can notice a qualitatively satisfactory agreement between the photophysical picture of the reaction resulting from the CASSCF calculations and that obtained at the CC2 level of theory (Figure 2). For the hydroxy and oxo tautomeric forms, the $n\pi^*$ state lies “vertically” below the corresponding $\pi\pi^*$ state. The PE profiles of the $n\pi^*$ and $\pi\pi^*$ excited states (similarly as the PE profile of the ground state) are bound with respect to elongation of the respective OH (Figure 3a) or NH (Figure 3b) distances.

At the OH (or NH) distances elongated by ca. 0.25 Å (with respect to the optimized geometries of the hydroxy and oxo minima) the PE profiles of the locally excited $n\pi^*$ and $\pi\pi^*$ states are intersected by a repulsive $\pi\sigma^*$ state. The energies of the LST points at these intersections provide an estimate of the barriers heights for nonadiabatic transitions from the optically populated FC area of PE surfaces to the “reactive” $\pi\sigma^*$ state. The intersections (visualized in Figure 3) can only provide an

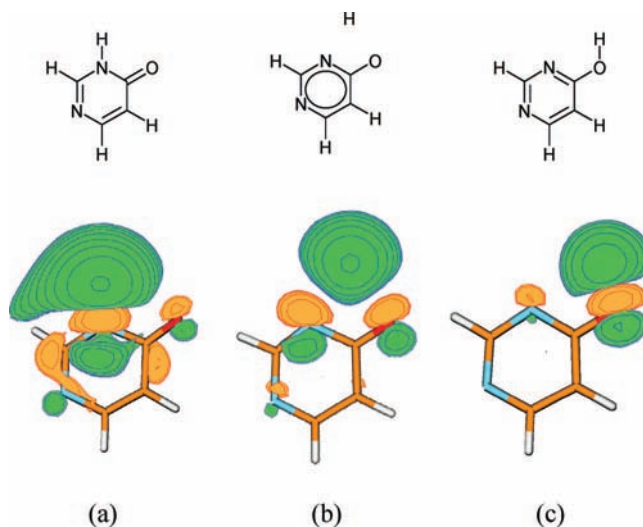


Figure 4. The σ^* natural orbitals obtained by a CASSCF calculation performed for (a) the oxo form; (b) a point at the intersection seam between the excited $\pi\sigma^*$ state and the ground state of the 4(3H)-pyrimidinone/4-hydroxypyrimidine system; and (c) the hydroxy form.

upper estimate for the barriers, since the real saddle-points have not been optimized. Moreover, the CASSCF method does not account for dynamical electron correlation effect which constitutes an important factor that determines topology of PE surfaces. Thus, results shown in Figure 3 can only provide a qualitative mechanistic picture of the investigated photophysical process.

After the nonadiabatic transition from the FC area to the PE surface of the $\pi\sigma^*$ state, the system evolves on the dissociative PE surface in the direction of its intersection seam with the ground state. In the area, where the OH and NH distances are greater than 2.0 Å (see the center of Figure 3) the $\pi\sigma^*$ and S_0 states become nearly isoenergetic. This picture is in qualitative agreement with the results obtained at the CC2 level (Figure 2), which predict (at OH and NH distances of ca. 2 Å) an extended seam of intersection between the $\pi\sigma^*$ and S_0 states.

The approximately biradical character of the $\pi\sigma^*$ state at the seam of the $\pi\sigma^*$ – S_0 intersection is also reflected by the shape of the σ^* natural orbital localized at the mobile hydrogen atom (see Figure 4). Whereas at the equilibrium geometries of the 4PMD (Figure 4a) and 4HPM (Figure 4c) tautomers its shape is typical of antibonding orbitals, at geometry with OH and NH distances equal 2.2 Å (Figure 4b) this orbital adopts a nearly spherical shape, which collapses to the 1s orbital of atomic hydrogen for larger NH/OH distances.

Experimental Picture. For the barriers, which the system has to surmount to access the $\pi\sigma^*$ state from the initially excited $\pi\pi^*$ and $n\pi^*$ states, only the upper limits were computationally estimated. On the basis of the computations carried out in the current work, an upper limit for the barrier (of about 0.8 eV) was predicted. Some more information on this subject can be derived from the experimental studies of the phototautomeric reaction in the 4PMD/4HPM system.

The origin of the S_0 – S_1 transition (the 0–0 transition) was observed at 30528 cm^{-1} (3.785 eV) for jet-cooled 4PMD.²¹ On the other hand, it was experimentally shown that the oxo \rightarrow hydroxy phototautomerism in this compound occurs upon irradiation of the monomers with UV ($\lambda = 308$ nm, 4.025 eV) monochromatic light.³ This suggests that the energy excess necessary to promote the phototautomeric reaction is no higher than 0.24 eV.

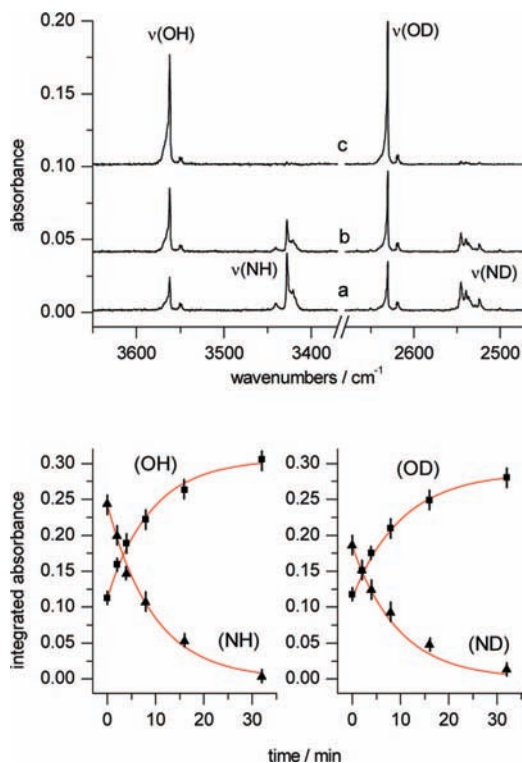


Figure 5. Progress of the phototautomeric oxo \rightarrow hydroxy reaction observed for nondeuterated and deuterated [at N(3) atom] **4PMD/4HPM** system. Monomers of both isotopologues were isolated in the same low-temperature Ar matrix (at 10 K). The matrix was irradiated with a high pressure HBO200 mercury lamp fitted with a UG11 (Schott) filter transmitting light with $\lambda > 270$ nm. Upper panel: fragments of the infrared spectra recorded (a) after deposition of the matrix; (b) after 4 min of UV irradiation; (c) after 32 min of UV irradiation. Lower panel: intensities of the bands due to $\nu(\text{OH})$, $\nu(\text{NH})$, $\nu(\text{OD})$ and $\nu(\text{ND})$ vibrations measured at the consecutive stages of the progress of the phototautomeric reaction.

Moreover, for the purpose of the present study, several experiments were carried out, in order to investigate the oxo \rightarrow hydroxy phototautomerism in an isotopologue of **4PMD/4HPM** with N(3)-H hydrogen atom substituted by deuterium (experimental details can be found in the Supporting Information). These experiments demonstrated that photoinduced deuteron transfer, analogous to the oxo \rightarrow hydroxy proton transfer in **4PMD/4HPM**, occurs also for the deuterated isotopomer. The relative time constants of proton-transfer and deuteron-transfer reactions were measured in an experiment on UV irradiation of an argon matrix containing monomers of nondeuterated as well as monomers of deuterated compound. For such a matrix, the conditions of UV-irradiation of nondeuterated and deuterated molecules were the same. The obtained results show that the rates of the UV-induced proton-transfer and deuteron-transfer reactions are very similar, with the proton transfer only slightly faster than the deuteron transfer (Figure 5). Based on these observations, one can conclude that the barriers for the proton movement in the excited states are rather low. Otherwise, in the case of high barriers, proton (or deuteron) tunneling would become a main rate-limiting factor and deuteration would substantially (by orders of magnitude) slow down the observed phototautomeric process.

Conclusions

In recent years, photoinduced hydrogen atom detachment processes (where H-atom is released by cleavage of the N–H

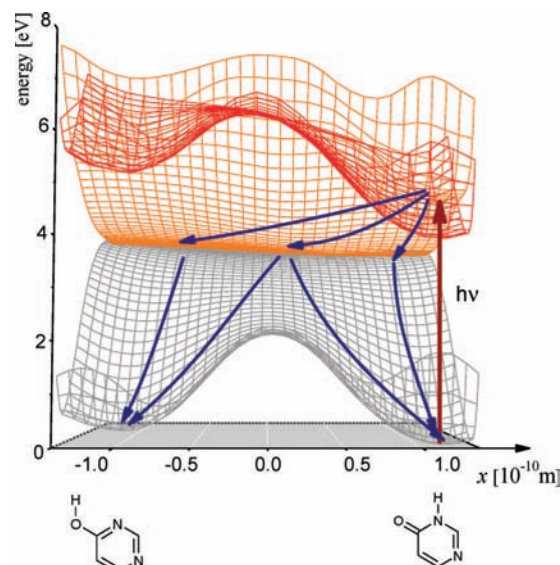


Figure 6. Graphical representation of the PIDA mechanism of the oxo \rightarrow hydroxy phototautomerism in the 4(3H)-pyrimidinone/4-hydroxypyrimidine system. Blue arrows show the possible paths of evolution of the system following UV excitation.

or O–H bonds) have been experimentally observed for a number of heteroaromatic compounds, such as pyrrole,^{28,30} phenol^{31,53} and indole.^{34,35} These experimental findings were inspired by theoretical calculations^{24,26,54} predicting that the photoinduced H-atom detachment should be driven by a repulsive $\pi\sigma^*$ state.

Within the current work, we postulate that an analogous mechanism can be used for a mechanistic explanation of the intramolecular phototautomerization in heteroaromatic systems, which have acidic and basic moieties not connected to each other by a hydrogen bond. We present a computational model showing that the phototautomerism, observed for a number of compounds with N–H and C=O groups in the α position (with respect to each other), might be treated as a subclass of the photochemical processes driven by repulsive $\pi\sigma^*$ states. In the postulated (PIDA) model, a molecule promoted by absorption of a UV quantum to a locally excited electronic state can (usually by crossing a low-energy barrier) internally convert to a PE surface of the $\pi\sigma^*$ state, which is repulsive with respect to the hydrogen atom detachment. On this PE surface, the system evolves toward the seam of intersection between the $\pi\sigma^*$ and the ground electronic states. This intersection seam is located at geometry points corresponding to significantly elongated N–H or O–H bonds. At such geometry, the system can be approximately treated as a biradical consisting of the departing hydrogen atom and the radical of the remaining molecular frame. In the gas or in the liquid phase, the excess of kinetic energy of the departing hydrogen atom may result in its real dissociation. In a rigid environment of a low-temperature noble-gas matrix, this reaction path is very unlikely due to spatial confinement, and the system returns to the ground-state PE surface due to nonadiabatic interactions at the points along the $\pi\sigma^*$ – S_0 intersection seam. By further dissipation of the excess of energy the system relaxes (on the ground electronic state PE surface) toward one of the two (oxo or hydroxy) ground-state minima. This may either restore the initial form of the reactant, if hydrogen attaches to the same heteroatom, or result in phototautomerization, if hydrogen attaches to another heteroatom of the molecular system (Figure 6). The barrierless bifurcation of the evolution of the system at the last of the above-mentioned stages allows a molecule to change its tautomeric form, in spite

of high-energy barriers separating the oxo and hydroxy tautomers in the ground and in the locally excited electronic states.

Acknowledgment. This work has been supported by the grant of the Interdisciplinary Center of Mathematical and Computer Modeling (ICM) of the University of Warsaw (Grant No. G29-11).

Supporting Information Available: Experimental Section providing information on the methods applied to record infrared spectra of matrix-isolated species and to induce the phototautomeric processes. Table S1 with the vertical excitation energies of the low-energy singlet excited states of 4-hydroxypyrimidine and 4(3*H*)-pyrimidinone calculated at the CC2, CASSCF and CASPT2 levels. This material is available free of charge via the Internet at <http://pubs.acs.org>.

References and Notes

- Nowak, M. J.; Fulara, J.; Lapinski, L. *J. Mol. Struct.* **1988**, *175*, 91.
- Lapinski, L.; Fulara, J.; Nowak, M. J. *Spectrochim. Acta, Part A* **1990**, *46*, 61.
- Lapinski, L.; Nowak, M. J.; Les, A.; Adamowicz, L. *J. Am. Chem. Soc.* **1994**, *116*, 1461.
- Gerega, A.; Lapinski, L.; Nowak, M. J.; Furmanchuk, A.; Leszczynski, J. *J. Phys. Chem. A* **2007**, *111*, 4934.
- Nowak, M. J.; Lapinski, L.; Fulara, J.; Les, A.; Adamowicz, L. *J. Phys. Chem.* **1992**, *96*, 1562.
- Lapinski, L.; Fulara, J.; Czerminski, R.; Nowak, M. J. *Spectrochim. Acta, Part A* **1990**, *46*, 1087.
- Maier, G.; Endres, J. *Eur. J. Org. Chem.* **2000**, 1061.
- Duvernay, F.; Trivella, A.; Borget, F.; Coussan, S.; Aycard, J. P.; Chiavassa, T. *J. Phys. Chem. A* **2005**, *109*, 11155.
- Duvernay, F.; Chatron-Michaut, P.; Borget, F.; Birney, D. M.; Chiavassa, T. *Phys. Chem. Chem. Phys.* **2007**, *9*, 1099.
- Duvernay, F.; Chiavassa, T.; Borget, F.; Aycard, J. P. *J. Phys. Chem. A* **2005**, *109*, 6008.
- Nowak, M. J.; Lapinski, L.; Fulara, J. *Spectrochim. Acta, Part A* **1989**, *45*, 229.
- Lapinski, L.; Nowak, M. J.; Fulara, J.; Les, A.; Adamowicz, L. *J. Phys. Chem.* **1990**, *94*, 6555.
- Vranken, H.; Smets, J.; Maes, G.; Lapinski, L.; Nowak, M. J. *Spectrochim. Acta, Part A* **1994**, *50*, 875.
- Gerega, A.; Lapinski, L.; Nowak, M. J.; Rostkowska, H. *J. Phys. Chem. A* **2006**, *110*, 10236.
- Gerega, A.; Lapinski, L.; Reva, I.; Rostkowska, H.; Nowak, M. J. *Biophys. Chem.* **2006**, *112*, 123.
- Ivanov, A. Yu; Plokhhotnichenko, A. M.; Izvekov, V.; Sheina, G. G. *J. Mol. Struct.* **1997**, *408/409*, 459.
- Matsuda, Y.; Ebata, T.; Mikami, N. *J. Chem. Phys.* **1999**, *110*, 8397.
- Li, Q.-S.; Fang, W.-H.; Yu, J.-G. *J. Phys. Chem. A* **2005**, *109*, 3983.
- Nimlos, M. R.; Kelley, D. F.; Bernstein, E. R. *J. Phys. Chem.* **1989**, *93*, 643.
- Sinha, R. K.; Pradhan, B.; Wategaonkar, S.; Singh, B. P.; Kundu, T. *J. Chem. Phys.* **2007**, *126*, 114312.
- Tsuchiya, Y.; Tamura, T.; Fujii, M.; Ito, M. *J. Phys. Chem.* **1988**, *92*, 1760.
- Sobolewski, A. L.; Domcke, W. *Chem. Phys. Lett.* **1999**, *315*, 293.
- Sobolewski, A. L.; Domcke, W. *Chem. Phys.* **2000**, *259*, 181.
- Sobolewski, A. L.; Domcke, W.; Dedonder-Ladeux, C.; Jouvret, C. *Phys. Chem. Chem. Phys.* **2002**, *4*, 1093.
- Lan, Z.; Domcke, W.; Vallet, V.; Sobolewski, A. L.; Mahapatra, S. *J. Chem. Phys.* **2005**, *122*, 224315.
- Vallet, V.; Lan, Z.; Mahapatra, S.; Sobolewski, A. L.; Domcke, W. *J. Chem. Phys.* **2005**, *123*, 144307.
- Blank, D. A.; North, S. W.; Lee, Y. T. *Chem. Phys.* **1994**, *187*, 35.
- Wei, J.; Kuczmann, A.; Riedel, J.; Renth, F.; Temps, F. *Phys. Chem. Chem. Phys.* **2003**, *5*, 315.
- Cronin, B.; Nix, M. G. D.; Qadiri, R. H.; Ashfold, M. N. R. *Phys. Chem. Chem. Phys.* **2004**, *6*, 5031.
- Lippert, H.; Ritze, H.-H.; Hertel, I. V.; Radloff, W. *ChemPhysChem* **2004**, *5*, 1423.
- Tseng, C.-M.; Lee, Y. T.; Ni, C.-K. *J. Chem. Phys.* **2004**, *121*, 2459.
- Ashfold, M. D. R.; Cronin, B.; Devine, A. L.; Dixon, R. N.; Nix, M. G. D. *Science* **2006**, *312*, 1637.
- Lan, Z.; Dupays, A.; Vallet, V.; Mahapatra, S.; Domcke, W. *J. Photochem. Photobiol. A* **2007**, *190*, 177.
- Lin, M. F.; Tseng, C.-M.; Lee, Y. T.; Ni, C.-K. *J. Chem. Phys.* **2005**, *123*, 124303.
- Nix, M. G. D.; Devine, A. L.; Cronin, B.; Ashfold, M. N. R. *Phys. Chem. Chem. Phys.* **2006**, *8*, 2610.
- Sobolewski, A. L. *Chem. Phys. Lett.* **1993**, *211*, 293.
- Sobolewski, A. L.; Adamowicz, L. *Chem. Phys.* **1996**, *213*, 193.
- Sobolewski, A. L.; Adamowicz, L. *J. Phys. Chem.* **1996**, *100*, 3933.
- Sobolewski, A. L.; Domcke, W. *J. Phys. Chem. A* **2007**, *111*, 11725.
- Christiansen, O.; Koch, H.; Jørgensen, P. *Chem. Phys. Lett.* **1995**, *243*, 409.
- Hättig, C.; Weigend, F. *J. Chem. Phys.* **2000**, *113*, 5154.
- Köhn, A.; Hättig, C. *J. Chem. Phys.* **2003**, *119*, 5021.
- Weigend, F.; Häser, M. *Theor. Chem. Acc.* **1997**, *97*, 331.
- Ahlrichs, R.; Bär, M.; Häser, M.; Horn, H.; Kölmel, C. *Chem. Phys. Lett.* **1989**, *162*, 165.
- Roos, B. O. *Advan. Chem. Phys.* **1987**, *69*, 399.
- MOLPRO is a package of ab initio programs written by Werner, H.-J. and Knowles, P. J. with contributions from Lindh, R.; Manby, F. R.; Schütz, M.; Celani, P.; Korona, T.; Mitrushenkov, A.; Rauhut, G.; Adler, T. B.; Amos, R. D.; Bernhardsson, A.; Berning, A.; Cooper, D. L.; Deegan, M. J. O.; Dobbyn, A. J.; Eckert, F.; Goll, E.; Hampel, C.; Hetzer, G.; Hrenar, T.; Knizia, G.; Köppl, C.; Liu, Y.; Lloyd, A. W.; Mata, R. A.; May, A. J.; McNicholas, S. J.; Meyer, W.; Mura, M. E.; Nicklass, A.; Palmieri, P.; Pflüger, K.; Pitzer, R.; Reiher, M.; Schumann, U.; Stoll, H.; Stone, A. J.; Tarroni, R.; Thorsteinsson, T.; Wang, M.; Wolf, A., version 2008.1.
- Dunning, T. H. *J. Chem. Phys.* **1989**, *90*, 1007.
- Møller, C.; Plesset, M. S. *Phys. Rev.* **1934**, *46*, 618.
- Nowak, M. J.; Szczepaniak, K.; Barski, A.; Shugar, D. *J. Mol. Struct.* **1980**, *62*, 47.
- Beak, P.; Fry, F. S., Jr.; Lee, J.; Steele, F. *J. Am. Chem. Soc.* **1976**, *98*, 171.
- Kistler, K. A.; Matsika, S. *J. Phys. Chem. A* **2007**, *111*, 8708.
- Sobolewski, A. L.; Woywod, C.; Domcke, W. *J. Chem. Phys.* **1993**, *98*, 5627.
- Tseng, C.-M.; Lee, Y. T.; Lin, M. F.; Ni, C.-K.; Liu, S. Y.; Lee, Y. P.; Xu, Z. F.; Lin, M. C. *J. Phys. Chem. A* **2007**, *111*, 9463.
- Abe, M.; Ohtsuki, Y.; Fujimura, Y.; Lan, Z.; Domcke, W. *J. Chem. Phys.* **2006**, *124*, 224316.